JOURNAL OF CHEMOMETRICS
J. Chemometrics 2002; **16**: 329–338
Published online in Wiley InterScience (www.interscience.wiley.com). DOI: 10.1002/cem.726

Monitoring of a batch organic synthesis by near-infrared spectroscopy: modeling and interpretation of three-way data

Paul Geladi* and Jennie Forsström†

Department of Chemistry, Umeå University, SE-901 87 Umeå, Sweden

Received 14 February 2001; Revised 29 January 2002; Accepted 12 February 2002

Three-way data of the type batch × time × NIR wavelength were obtained by NIR spectroscopic multivariate monitoring of an organic synthesis as a batch process. The model synthesis, an ester synthesis, was carried out as an experimental design. Unexpected technical problems caused a blocking effect that forced a modification of the design. After preprocessing of a reduced three-way array, the spectral data in the three-way array were subjected to parallel factor analysis (PARAFAC). The loadings from this analysis could be interpreted and explained as a function of the synthesis studied. For the spectral interpretation, spectra of pure chemicals were needed. The paper is an illustration of what can be done with three-way modeling in order to increase the understanding of a reaction, and it attempts to show how the results can be interpreted and presented. The data sets are available from the authors. Copyright © 2002 John Wiley & Sons, Ltd.

KEYWORDS: three-way data; batch organic synthesis; PARAFAC; near-infrared spectra; Savitzky–Golay transform; blocking; multiplicative scatter correction; experimental design

1. INTRODUCTION

In chemistry, it may sometimes be important to follow a batch synthesis reaction and to identify the products in the reaction mixture during different stages of the reaction. Near-infrared fiber optic monitoring is a very easy and fast way of obtaining rich spectral information. When many batch organic reactions are monitored over time by near-infrared (NIR) spectroscopy, the results form a batch × time × wavelength three-way array that can be analyzed by PARAFAC, as described by Geladi and Åberg [1]. The reference also mentions earlier literature on the subject of batch synthesis/process monitoring, as does a recent reference by Smilde [2]. The model synthesis studied in this paper is the production of isoamyl acetate by a simple esterification from isoamyl alcohol and acetic acid at the boiling point of the reaction mixture. The reaction uses *p*-toluenesulfonic acid as a catalyst. The water is systematically removed by azeotropic distillation with benzene, and this moves the equilibrium towards the ester. The reaction in itself is just a simple textbook example, and the emphasis in the paper is on the chemometric aspects of the data analysis, but the concepts are easily transferred to reactions of more industrial relevance. An advantage of a simple model reaction is that all the results and the raw data can be made available to others without problems of confidentiality. The paper also gives insights in how to solve expected (noise, baseline effects) and unexpected (block effect) problems before the final analysis can be presented.

Eleven reactions were carried out as a 3^2 design with two extra center points. Spectra of pure chemicals and mixtures were measured for the purpose of assisting in spectral interpretation. The NIR spectra were taken with a fiber optic probe every 3 min for almost 2 h, giving 40 points in time. The NIR spectra originally contained 1050 wavelengths, every 2 nm from 400 to 2498 nm. Together the data form an $11 \times 40 \times 1050$ three-way array that can be analyzed by three-way factor analysis methods. This array is shown schematically in Figure 1. The data can also be analyzed by two-way analysis methods, but this is rather trivial and therefore not elaborated here. Earlier versions of the batch synthesis reaction were not very satisfactory for a number of reasons, and the reaction as described by Geladi and Åberg [1] was improved in many ways:

- change of catalyst from solid to dissolved;
- change of water removal method from molecular sieve (solid) to azeotropic distillation in benzene (dissolved);
- better control of the temperature;
- more frequent measurement over time;
- a smaller gap for the fiber optic transflectance probe, avoiding spectrum saturation;
- one experienced operator carries out all the reactions;

*Correspondence to: P. Geladi, Department of Chemistry, Umeå University, SE-901 87 Umeå, Sweden.
E-mail: paul.geladi@chem.umu.se
†Current address: Department of Natural and Environmental Science, Mid Sweden University, SE 85170 Sundsvall, Sweden.

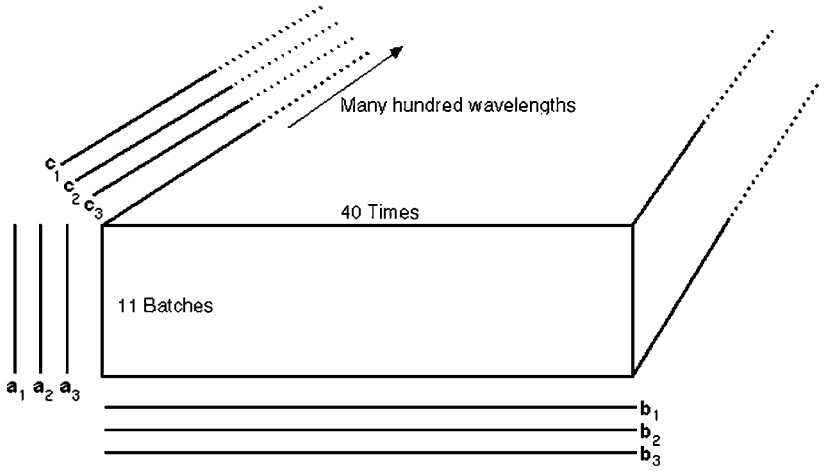

Figure 1. Three-way data set of 11 batches × 40 times × 1050 wavelengths. PARAFAC decomposes the array into A-loadings, B-loadings and C-loadings. A pseudorank = 3 solution is shown here. The A-loadings explain differences between the batches, the B-loadings can be interpreted as time profiles and the C-loadings can be interpreted as spectra.

- measuring of pure chemicals and known mixtures at reaction temperature for comparison.

The improvements in the reaction were intended to give better precision and therefore an improved intepretation of the three-way analysis and model.

Three-way arrays can be decomposed by factor analytical methods. These methods are not the same as those for two-way arrays. A parallel factor analysis (PARAFAC) or CANDECOMP decomposition decomposes a three-way array into A-, B- and C-loadings (see also Figure 1). The methods are also described by Geladi [3], Smilde [4] and Bro [5] and in the books by Law *et al.* [6] and Coppi and Bolasco [7]. A whole issue of the *Journal of Chemometrics* on three-way analysis was recently published under the editorship of Andersson and Bro [8]. The PARAFAC decomposition is done as follows:

$$x_{ijk} = a_{i1}b_{j1}c_{k1} + a_{i2}b_{j2}c_{k2} + \ldots + a_{iR}b_{jR}c_{kR} + e_{ijk} \qquad (1)$$

where x_{ijk} is an element of the three-way array $\underline{X}$, r is the index of the pseudorank, $r = 1, \ldots, R$, a_{ir} are elements of the A-loadings, b_{jr} are elements of the B-loadings, c_{kr} are elements of the C-loadings and e_{ijk} is the residual, an element of the three-way array $\underline{E}$.

The PARAFAC decomposition is done for a chosen number of components, the pseudorank, and this pseudorank can give information about the system under study. The A-, B- and C-loadings from PARAFAC can be shown as line plots (loading value against wavelength) or as scatter plots. In this way they reveal information about the reaction. As shown in Figure 1, the A-loadings explain the batch mode, the B-loadings explain the time mode and the C-loadings explain the spectral mode. Once a good pseudorank is chosen, the PARAFAC decomposition is unique and can give curve resolution results without a need for extra constraints [4,5]. Allosio *et al.* [9] have published work on the three-way analysis of NIR spectra by PARAFAC modeling.

It was shown by Geladi and Åberg [1] that a PARAFAC decomposition of pseudorank three could give meaningful information about the reaction and its products. The time profiles of components 1 and 2 could be interpreted as disappearing reagents and emerging reaction product, the spectral profiles could be interpreted by comparison with pure chemical data, and the batch profiles were related to reaction rate. The third PARAFAC component could be interpreted as a peak broadening because of protonation, probably of the acetic acid. An important goal of the present paper is refining the synthesis and trying to extract and explain more PARAFAC components.

Near-infrared spectra are overtones of the infrared spectral region. They have wider peaks than infrared spectra [10,11]. NIR spectra are not always measured in transmission mode with constant path length, and this contributes to the difficulties in interpretation. It is generally assumed that the interpretation of NIR spectra is not as easy as that of infrared spectra, where distinct peaks are representative for functional groups. This makes it difficult to chemically intepret the PARAFAC loadings [1] by visual inspection or comparison with tables, as is usual in infrared spectroscopy. The solution used in this paper is comparison with pure chemical spectra measured with the same fiber optic probe and in the same conditions as the actual reaction.

For NIR data it may be necessary to correct for baseline effects before building a model. This is called pretreatment and is used frequently. Multiplicative scatter correction (MSC) [12] and taking derivatives using the Savitzky–Golay transform (SGT) [13] were applied to the NIR spectra. The SGT transform is a smoothing derivation [14].

The goal of the whole study was to show that PARAFAC loadings can be interpreted meaningfully to understand the reaction better. The present paper only discusses interpretation of the PARAFAC model, not the building of control charts or the prediction of future batches as discussed by Smilde [2].

2. EXPERIMENTAL

2.1. The esterification reaction and experimental design

The general reaction is

$$C_5H_{11}OH + CH_3CO-OH \overset{H^+}{\longleftrightarrow} C_5H_{11}O-COCH_3 + H_2O$$

The esterification reaction is a nucleophilic substitution by the alcohol on a protonated carboxylic acid [15]. The use of an acid catalyst is necessary. The reaction is reversible as a hydrolysis, and this hydrolysis is also catalyzed by the acid. Therefore it is important to have a surplus of one of the reagents and/or remove the water. When measuring on-line with NIR, it is important to avoid suspended solid materials that foul the transflectance probe. A number of different reactions were tried by Forsström [16], but these are not elaborated here. The best version was the use of *p*-toluenesulfonic acid as a catalyst combined with azeotropic distillation of the water with benzene, also called the Dean–Stark trap method [17]. Each reaction used 90 ml of benzene and 125 ml as the sum of acetic acid and isoamyl alcohol. The reaction was carried out under reflux in a 500 ml flask at 85 °C. Different batches were tried as runs in a 3^2 experimental design with two extra center points. The factors were reactant ratio and amount of catalyst. The reagents are shown in Table I. The design used is given in Table II. NIR spectra of pure chemicals and known mixtures were measured at 85 °C for easier spectral interpretation. A list is given in Table III. All the spectra in this table are means of six replicates. The mixtures were chosen to represent the spectra measured during the reactions as well as possible.

2.2. NIR measurement

The NIR fiber optic transflectance probe was used with a gap between fiber and mirror of 5 mm, because earlier experiments [18] had shown a tendency of detector saturation at certain wavelengths with larger gaps. Reflection from the probe mirror in air was used as the blank. The transflectance probe was left in the reaction mixture and a spectrum was recorded every 3 min. NIR spectra were measured using an NIRSystems 6500 spectrometer. Spectra were recorded in the wavelength range of 400–2498 nm, every 2 nm, with 32 scans per spectrum. Vision software of Foss was used for this purpose [19]. Spectra were recorded for two purposes: (1) the design as in Table II, giving an $11 \times 40 \times 1050$ array for PARAFAC analysis, and (2) spectra for the pure chemicals as in Table III for interpretation purposes.

2.3. Software

All calculations were done in MATLAB and in the PLS-Toolbox 2.0 for MATLAB [20,21].

Table II. Experimental design used ($3^2 + 2$ center points). Reactant ratio is given as mole acetic acid/mol isoamyl alcohol. Catalyst is given in grams added. The experiments with* form a Koshal design. No separate response is measured. The responses are taken from the PARAFAC loadings

Exp. #	Ratio	Catalyst	Run order
1*	1	0.15	10
2	1.5	0.15	5
3	2	0.15	1
4*	1	0.45	7
5	1.5	0.45	4
6	2	0.45	2
7*	1	0.75	9
8*	1.5	0.75	11
9*	2	0.75	8
10*	1.5	0.45	6
11	1.5	0.45	3

3. RESULTS AND DISCUSSION

The experimental design had 11 batch reactions as runs. In each batch reaction a 40 (times) $\times$ 1050 (wavelengths) matrix was generated. A simple PCA on the matricized array (a 440×1050 matrix) showed an unexpected block effect. This block effect was identified, and this resulted in the discarding of some of the batch data. Visual inspection of derivative spectra showed empty and noisy regions in the spectra, and these were removed by cropping. The resulting $6 \times 40 \times 776$ data array was analyzed by PARAFAC, and the resulting loadings were interpreted. The A-loadings were interpreted as responses for the experimental design and as scatter plots. The C-loadings were interpreted by their position in multivariate space together with the pure chemical spectra. The B-loadings were interpreted as line and scatter plots.

3.1. Block effect

The batch syntheses as in the experimental design of Table II were carried out and the runs form an $11 \times 40 \times 1050$ three-way array. This array can also be reorganized into a 440×1050 matrix. It is often instructive to do a simple principal component analysis of the obtained results in order to detect outliers and unexpected groupings in the data. The PCA model is

$$\mathbf{X} = \mathbf{T}\mathbf{P}^{\mathrm{T}} + \mathbf{E} \qquad (2)$$

where $\mathbf{X}$ is the data matrix, often mean-centered, $\mathbf{T}$ is the matrix whose columns are formed by the principal component scores $\mathbf{t}_1\mathbf{t}_2$, …, $\mathbf{P}$ is the matrix whose columns are formed by the principal component loadings $\mathbf{p}1$, $\mathbf{p}_2$, …, and $\mathbf{E}$ is the residual.

Table I. Chemicals used and amounts

1.	Acetic acid (PA), Merck, CAS# 64-19-7	1–2 molar ratio; see Table II
2.	Benzene, Sigma-Aldrich, CAS# 71-43-2	90 ml
3.	Isoamyl alcohol (PA), Merck, CAS# 123-51-3	Sum of 1 and 3 = 125 ml
4.	*p*-Toluenesulfonic acid, Acros, CAS# 104-15-4	0.15–0.75 g; see Table II
5.	Isoamyl acetate (Purum), Kebo, CAS# 123-92-2	(Only used to identify the spectrum)

Table III. Pure components and mixtures measured. Six replicates were used to form mean spectra

Composition	Also called
C_6H_6	Benzene
$C_5H_{11}O—COCH_3$	Ester
$C_5H_{11}O—COCH_3/C_6H_6$	Ester/benzene
$CH_3CO—OH$	Acid
$CH_3CO—OH/C_6H_6$	Acid/benzene
$C_5H_{11}OH$	Alcohol
$C_5H_{11}OH/C_6H_6$	Alcohol/benzene
Reaction mixture	Mixture
Reaction mixture/C_6H_6	Mixture/benzene
H_2O	Water

Principal component analysis of the 440 × 1050 two-way matrix (wavelength-wise mean-centered) gave three components with sum of squares (SS) of 95.4%, 2.5% and 1.8% respectively. The score plots showed an unexpected block effect. This can be seen clearly in Figure 2, the t_1–t_2 score plot. The first principal component dimension separates two groups of spectra: batches 1–5 and batches 6–11. The loading plot for the corresponding first component is shown as a line plot in Figure 3 and called 'block' loading. It definitely has the look and peaks of an NIR spectrum. The huge (95.5% SS) block effect causes the first loading vector to incorporate the differences between the blocks, i.e. the spectrum of what is different between early and late batches. The second component in Figure 2 shows how the variance is larger for early than for late batches.

3.2. Explaining the block effect

Visual comparison of the loading in Figure 3 with spectra of pure chemicals or known mixtures was not conclusive. Therefore a data matrix combining the 10 spectra as given in Table III and the 'block' loading as rows was made. All the spectra (rows) in this 11 × 1050 matrix were normalized to length one. Principal component analysis can be applied to this matrix. Score plots from PCA are difficult to interpret, because many of them ($\mathbf{t}_1$–$\mathbf{t}_2$, $\mathbf{t}_1$–$\mathbf{t}_3$, $\mathbf{t}_2$–$\mathbf{t}_3$, $\mathbf{t}_1$–$\mathbf{t}_4$, …) have to be studied together. Clustering takes into account all dimensions of the data. Clustering is very difficult on large data sets, so the 11 principal component scores of the 11 × 1050 variable-wise mean-centered matrix were subjected to *k*-means clustering [21], and the resulting dendrogram is given in Figure 4. The nearest neighbors of the 'block' loading are the ester, the ester in benzene, and benzene. This leads to the assumption that these products have contaminated the probe and thereby are responsible for this block effect. The clustering could have been done with less than 11 principal components, but one should remember that the higher components are less important (have a smaller contribution to the sum of squares), so they are automatically downweighted.

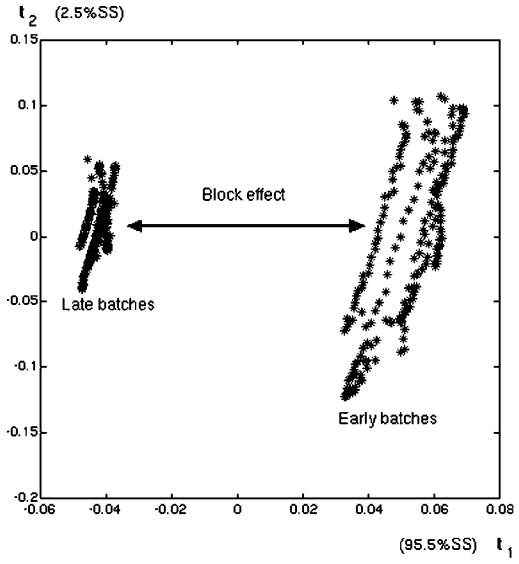

Figure 2. Score plot of first and second normalized scores of 440 × 1050 mean-centered data matrix. A clear block effect separating early (1–5) and late (6–11) batches is seen in the huge first component.

3.3. Reducing the design

Because the block effect comes from interfering chemicals contaminating the probe, it cannot be removed by simply using baseline and slope corrections. The transflectance spectra are always measured against a 100% reflectance standard, usually by holding the clean probe in air. The spectra before and after the blocking event therefore have different reference standards. Because of this, it was decided to work only with the second block, because it is larger and because also the pure spectra were measured in the second block. By coincidence, the six batches still form an experimental design, now a three-level two-factor Koshal design (see Figure 5) as explained by Meyers and Montgomery [22]. This design still allows the calculation of quadratic or interaction coefficients in the regression model; however, the intrepretation of the coefficients is less clear than for the original 3^2 design, because fewer degrees of freedom are left for the residual.

3.4. Pretreatment and cropping of spectra

It was shown earlier by Geladi and Åberg [1] that PARAFAC analysis of the raw spectra does not work very well, and the present data gave the same result. Therefore Savitzky–Golay first derivative (window size 31, fourth-order polynomial) [13] was used on the MSC-corrected spectra. The spectra of one batch are given in Figure 6. It was decided to crop the wavelength range to 550–2100 nm in order to avoid spectral regions having only baseline or noise. The result is a 6 × 40 × 776 array with only the batches measured after the block effect.

3.5. PARAFAC analysis

The 6 × 40 × 776 array gave a stable four-component PARAFAC model. Models of lower pseudorank were unsatisfactory because they had too low a percentage of the sum of squares explained, whilst those of higher pseudorank gave noisy loadings. The PARAFAC results are given in Table IV. The model explains 99% of the total sum of squares. The sum of the individual sums of squares of the four components is also 99%. There is a misconception in the literature that cross-validation should always be used in data analysis. Cross-validation is just one of many validation

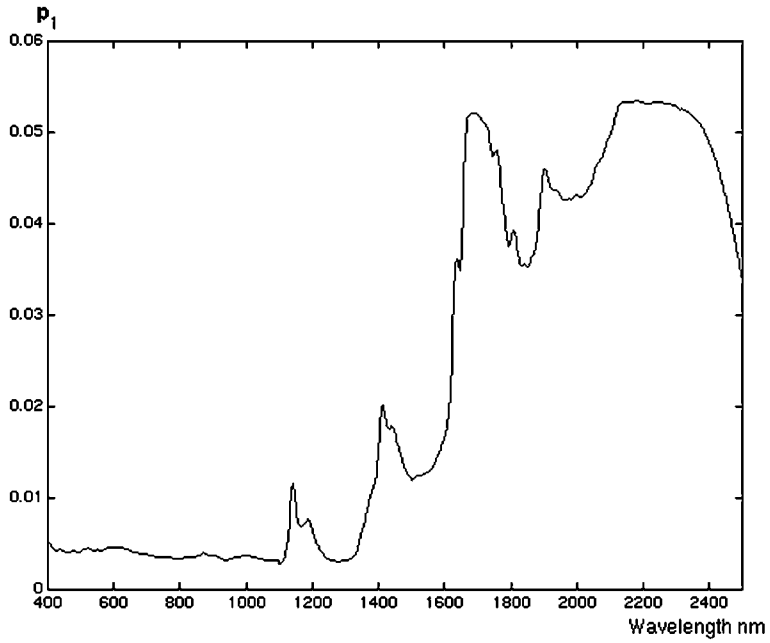

Figure 3. First loading of mean-centered 440 × 1050 matrix. A spectral interpretation of this loading indicates what went wrong to cause the block effect. It is therefore called 'block' loading.

tools and is often used out of laziness, because most software packages have it as a built-in default. In the present study the validation was done by interpretation of the total model SS and of the obtained loadings. For larger data sets (more batches), other validation criteria could be more useful.

Two-way curve resolution models are forced to use extra constraints for obtaining uniqueness. Often non-negativity of spectra and concentrations is used. The PARAFAC model is unique (except for sign flipping; see Equation (3) below), even when no non-negativity constraints are possible because of the use of derivative spectra. The PARAFAC model is unique for the data it is used on, but some subjective decisions have to be made in making the three-way array: to use MSC or not; choice of parameters for the Savitzky–Golay transform; use of first or second derivative; choice of wavelength range. The different choices gave different PARAFAC models, but with the same pseudorank and with a very similar interpretation. Once the model is determined, the PARAFAC A-, B- and C-loadings have to be intepreted, first separately and then together.

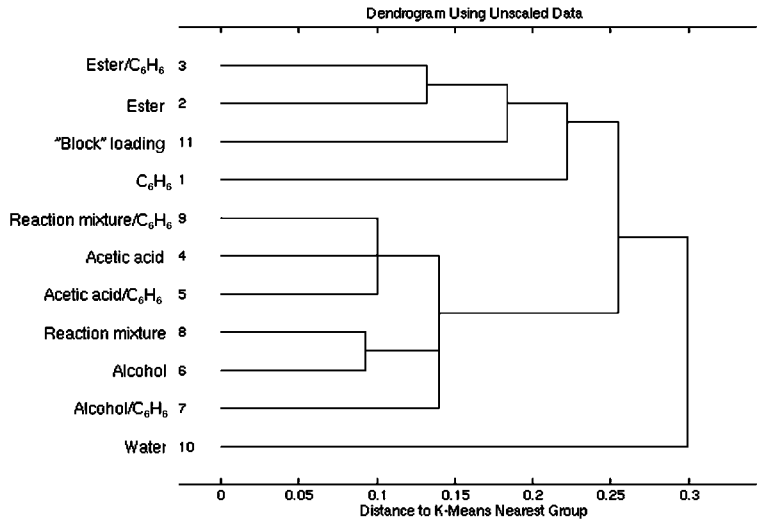

Figure 4. Dendrogram of pure chemicals and mixtures in Table III and 'block' loading. The dendrogram was calculated on the 11 PCA scores by the *k*-means method.

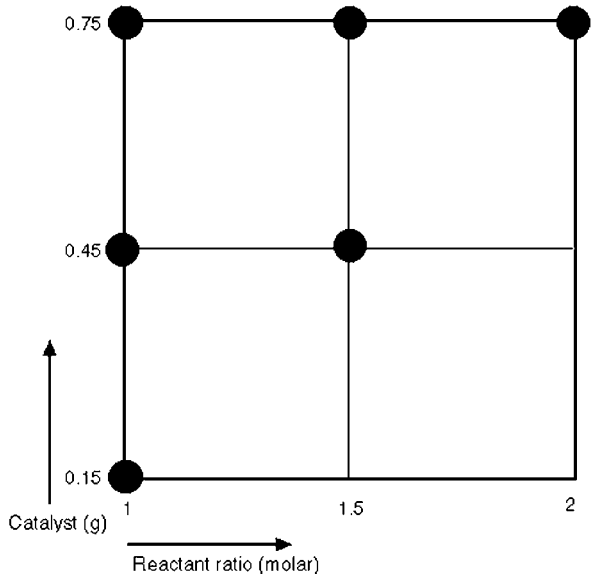

Figure 5. Reduced 3^2 design or three-level two-factor Koshal design. The amount of catalyst is flipped compared to the designs given in the literature.

The PARAFAC model in Equation (1) can be rewritten as

$$x_{ijk} = a_{i1}(-1)b_{j1}(-1)c_{k1} + (-1)a_{i2}(-1)b_{j2}c_{k2} + \ldots + (-1)a_{iR}b_{jR}(-1)c_{kR} + e_{ijk} \quad (3)$$

PARAFAC models are unique except for the sign of the loading vectors. This means that any pair of loading vectors can be flipped in sign and still give exactly the same model. It is sometimes necessary to use this possibility to get better understanding of the loadings.

Table IV. Results of PARAFAC model for $6 \times 40 \times 776$ array as sums of squares (SS)

Component number	% SS	SS
1	62	2.73
2	18	0.78
3	16	0.71
4	3.2	0.14
Model	99.2	4.38
Residual	0.8	0.038
Total	100	4.42

3.6. The A-loadings (batches)

The experiment is an experimental design with six runs and a 40×776 matrix of responses for each run. The responses for the design are matrices, but they can be reduced drastically to the A-loadings. The reduced 3^2 design and the Koshal design give the same fit, but different interpretation of the coefficients, because the reduced 3^2 design gives less correlation between the coefficients. Results for the analysis of the latter design are given in Table V. The regression model built is

$$a = b_0 + b_1x_1 + b_2x_2 + b_{12}x_1x_2 + \varepsilon \quad (4)$$

where a is an A-loading, the b_i are regression coefficients, ε is the residual, x_1 is the molar ratio and x_2 is the amount of catalyst, both in coded values. Two of the four obtained A-loadings give regression models with a high R^2, and in one of them the molar ratio is a significant coefficient. Interpreta-

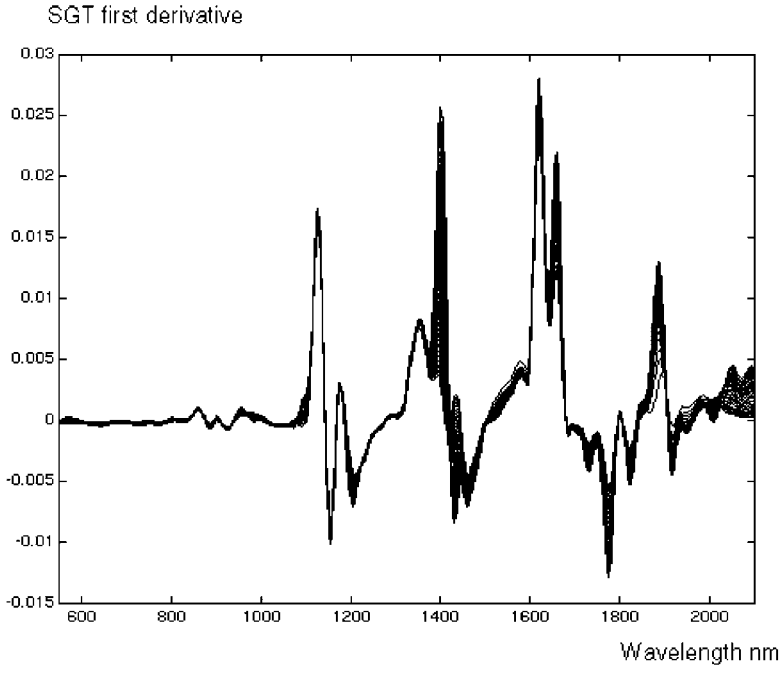

Figure 6. MSC-corrected, Savitzky–Golay first-derivative spectra of one batch. The wavelength regions 400–550 and 2100–2500 nm showed only baseline and noise and were removed.

Table V. Analysis of reduced 3^2 design with four PARAFAC A-loadings as responses. Values with # indicate a model without interaction term.* means 95% confidence interval;** means 99% confidence interval

Response number	R^2	Significant coefficients
1	0.40	None
2	0.97	Molar ratio*
3	0.95	None
4	0.77	None
2#	0.92	Molar ratio**
3#	0.94	Molar ratio*

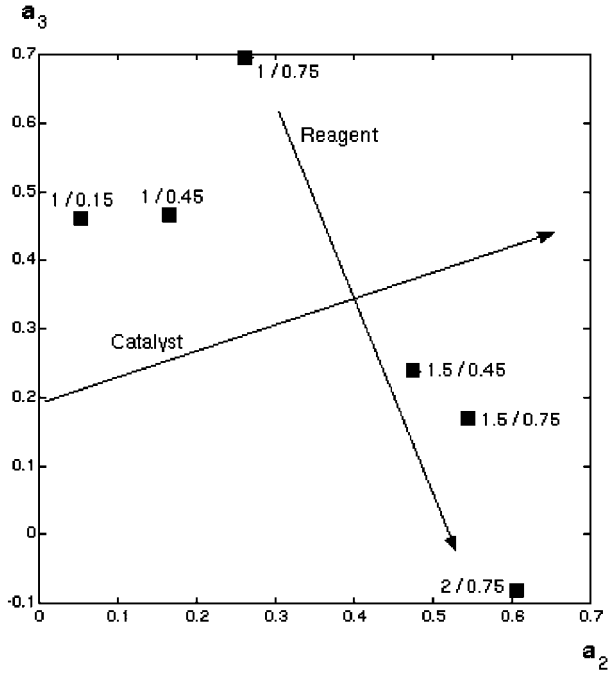

Figure 7. Loading plot of $\mathbf{a}_2$ and $\mathbf{a}_3$ showing effect of amount of catalyst and reagent ratio. Each point in the plot shows a run in the design as molar ratio/amount of catalyst. Arrows approximately show important directions in the plot: increasing reagent ratio and (less pronounced, but present) increasing amount of catalyst.

tion of the designs is hampered by the fact that only two degrees of freedom are available for the residual and that the design is not very orthogonal. Models were also calculated without the interaction term of Equation (2). They have three degrees of freedom for the residual. In this case both the second and third A-loadings get significant factors for the molar ratio. The conclusion of all this is that two of the A-loadings ($\mathbf{a}_2$ and $\mathbf{a}_3$) can be used to build design models and that in these models the factor 'molar ratio' is important. The large first component (62% of the total SS) and the small fourth component (3.2% of the total SS) are not dependent on the design. Figure 7 shows the $\mathbf{a}_2$–$\mathbf{a}_3$ loading plot. In this plot the importance of molar ratio and catalyst amount is seen for the second and third PARAFAC components. Other plots of the A-loadings did not show as much relationship to the design.

3.7. The C-loadings (spectra)

The C-loadings represent the spectral data, after spectral pretreatment and cropping to 776 wavelengths ranging from 550 to 2100 nm. In Reference [1], some of the loadings could be identified visually by comparison with pure component and mixture spectra. For the present example the C-loadings are compared with those of pure components and mixtures as given in Table III. For this purpose the pure component spectra needed to undergo the same pretreatment as those in the three-way array: MSC, SGT first derivative, cropping. The result was a 14×776 matrix, where the first 10 objects (rows) were known mixtures as in Table III and objects 11–14 were the four C-loadings. All object vectors in this matrix were normalized to length one, because the objective was to compare shapes and not sizes. This matrix was subjected to PCA after wavelength-wise mean-centering, giving components explaining 33%, 24% and 19% of the total sum of squares. The scores $\mathbf{t}_1$–$\mathbf{t}_2$ are shown in Figure 8 as a scatter plot. One obvious observation is that the pure chemicals are not so close to the C-loadings as the chemicals dissolved in benzene. Other score plots using the third principal component $\mathbf{t}_3$ led to similar conclusions as the one in Figure 8 and are not included.

In the score plot of Figure 8, $\mathbf{c}_1$ is close to the reaction mixture in benzene and to the alcohol in benzene, while c_3 is close to the ester in benzene and to pure benzene. This was also confirmed by visual inspection. It can be concluded that $\mathbf{c}_1$ represents the reaction mixture and that $\mathbf{c}_3$ represents the final product. The $\mathbf{c}_4$ loading takes on an intermediate position. It is explained by its B-loading in the next subsection. The $\mathbf{c}_2$ loading is on its own in the score plot. Therefore this loading requires extra attention. It was decided to sign-invert the B- and C-loadings (as in Equation (3)) for this component. The $\mathbf{c}_2$ loading is given in Figure 9. The spectral profiles for first-derivative NIR spectra are not as nice in shape as the UV-vis spectra described by Gurden *et al.* [23], but a closer look showed that many parts could be identified. They are indicated in Figure 9. The peak at 1400 nm is from protonation of the acetic acid, giving a peak broadening, also described earlier [1]. This can also be seen in Figure 6. The part from 1600 nm is from the ever-present benzene. The part around 1100–1200 nm resembles the spectrum of isoamyl alcohol in benzene. The second A-loading $\mathbf{a}_2$ gave an experimental design model (Equation (2)) with a high R^2 and a significant positive coefficient for the acid/alcohol ratio. This helps in concluding that a large part of $\mathbf{c}_2$ is based on the protonation of acetic acid.

3.8. The B-loadings (Time)

The B-loadings present the evolution over time of the batches. They are shown in Figure 10. The $\mathbf{b}_1$ loading goes down and stabilizes after about 40 min. It shows how the initial reaction mixture is being used up. The loading $\mathbf{b}_2$ shows how the acetic acid is protonated after addition of the acid catalyst and then used up; it goes down steadily. This loading is below the zero line because of the sign inversion. The $\mathbf{b}_3$ loading shows how the final product is being

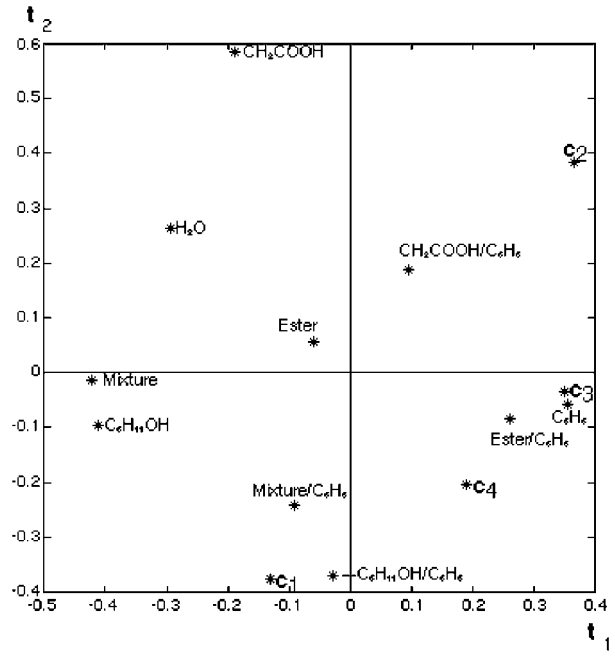

Figure 8. Score plot $\mathbf{t}_2$ against $\mathbf{t}_1$ for 14 × 776 matrix with pure components and mixtures of Table III and four C-loadings. Because of the orthogonality of the scores and the similarity of the eigenvalues, the plot is approximately Euclidean and distances can be interpreted as such.

generated. $\mathbf{b}_4$ is a small component. Looking back at the C-loadings aids in explaining $\mathbf{b}_4$. The position of $\mathbf{c}_4$ intermediate between $\mathbf{c}_1$ and $\mathbf{c}_3$ indicates that it is a compensation component that tries to explain the different reaction rates of the batches that show up in the data as non-trilinearity. It is also instructive to check the scatter plot of $\mathbf{b}_1$ and $\mathbf{b}_3$ in Figure 11. The trajectory of the reaction shows a fast move for the first 30 min and then a change in direction and a slower evolution after that. Because of the nature of the NIR spectra and the way the spectra are measured, it is not possible to apply the constraint that the sum of all the profiles should be constant.

4. CONCLUSIONS AND DISCUSSION

The batch reactions gave an 11 (batches) × 40 (times) × 1050 (wavelengths) array. A blocking effect was detected by PCA of the 440 × 1050 matrix, and it was determined from a loading plot that the blocking was due to contamination of the mirror of the transflectance probe by benzene and the ester. MSC combined with a first-derivative SGT was not able to take away the blocking effect. Therefore the batches were split and only the six after the blocking event were used. Some alternative ways of studying the blocking effect were tried, but these are not mentioned here because they did not improve the interpretation from PCA.

The spectra required an SGT derivative to allow the building of a PARAFAC model. Pure error data and studies of derived spectra suggested a cropping of the wavelength range, and the final array was 6 (batches) × 40 (times) × 776 (wavelengths). With this array a stable four-component PARAFAC model explaining 99% of the total sum of squares was obtained.

The PARAFAC loadings do not form a perfect curve resolution solution, but they are close enough to make meaningful interpretation possible. Near-infrared spectra are complicated and the pretreatment of the spectra probably results in PARAFAC loadings that are rotated versions of the ideal ones.

The loadings of the PARAFAC model were interpreted. The six batches formed a reduced 3^2 design, and significant regression models could be made for the $\mathbf{a}_2$ and $\mathbf{a}_3$ loadings, with a significant coefficient for the molar ratio factor. Also the $\mathbf{a}_2$–$\mathbf{a}_3$ scatter plot allowed an interpretation of the roles of

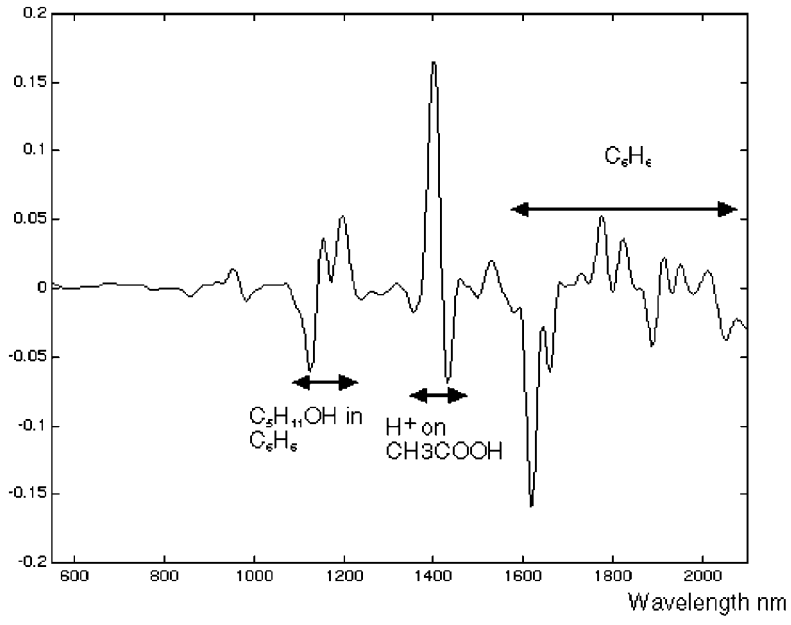

Figure 9. Line plot of $\mathbf{c}_2$ loading. Some identified regions are indicated.

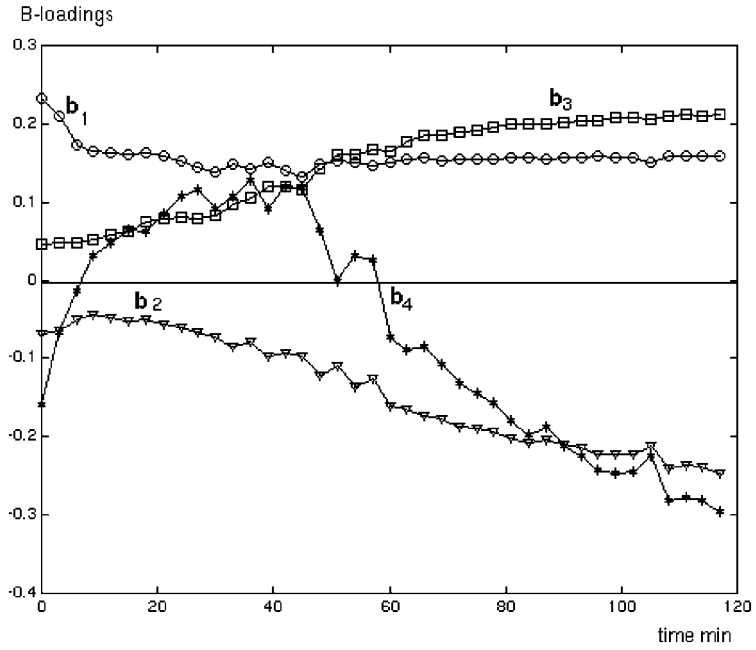

Figure 10. B-loadings in a line plot.

catalyst and molar ratio. The scatter plot of the A-loadings is quicker and easier to interperet than the regression models.

Spectral interpretation made use of a group of 10 pure component and known mixture spectra. In a score plot from PCA the C-loadings could be interpreted by similarity to mixture spectra. The $\mathbf{c}_1$ component resembled the reaction mixture in benzene; the $\mathbf{c}_3$ component resembled the reaction product in benzene. The $\mathbf{c}_4$ component was intermediate between these two. The $\mathbf{c}_2$ component could not be interpreted as resembling any of the pure mixtures, but

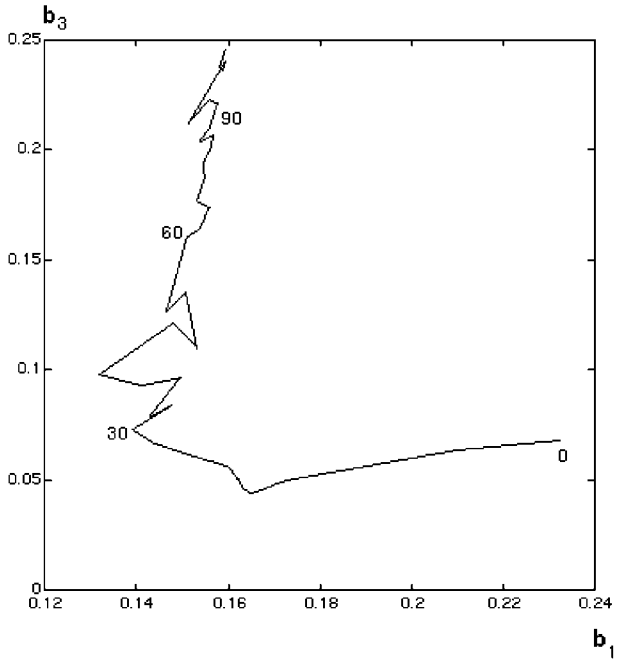

Figure 11. Scatter plot of $\mathbf{b}_1$ and $\mathbf{b}_3$. Some important times are indicated.

was identified as coming from a peak shift at 1400 nm caused by protonation of acetic acid. A sign inversion of the B- and C-loadings for component 2 was needed for this. The B-loadings can easily be interpreted once the C-loadings are known. The first B-loading shows how the initial reaction products are used up. The second B-loading shows the quick protonation of the acetic acid and slow removal of it. The third B-loading shows how the production of ester happens steadily. This also explains how the second and third A-loadings give good regression models for the reduced design. The $\mathbf{b}_4$ loading is small and can be interpreted as a compensation component. It compensates for the non-perfect trilinearity.

A possible chemical interpretation is that the inital reaction products ($\mathbf{c}_1$, $\mathbf{b}_1$) react quickly with the catalyst to give protonation of the acetic acid ($\mathbf{c}_2$). This happens during the first 30–40 min. After that the protonated acetic acid is used up ($\mathbf{c}_2$, $\mathbf{b}_2$, $\mathbf{a}_2$) and at the same time the ester is formed ($\mathbf{c}_3$, $\mathbf{b}_3$, $\mathbf{a}_3$). This reaction is slower and is still not completed after 2 h.

The use of benzene was necessary for the Dean–Stark method, but it was also an interferent, because benzene showed a strong NIR spectrum that was present in all spectra and influenced all C-loadings. In this respect the reaction in Reference [1] without the extra solvent was better.

For future studies it would be nice to remove the block effect and use the 11 batches together for stabilizing the PARAFAC solution even more. It would also be possible to use three-way regression with the pure chemical and mixture spectra as response variables. More cropping of the spectra may also produce even clearer results. Smoothing of the profiles over time is also a possible alternative. Alternatives to PARAFAC for further or future studies could be constrained PARAFAC, a Tucker model or a constrained Tucker model. For a larger data set (more batches) than the

one studied in the present paper, the difference between models may become clearer.

Acknowledgements

The authors would like to thank Pär Jonsson (Umeå University, Chemistry Dept) for helping with the spectrometer, Peter Åberg (Karolinska Institute, Dept of Clinical Physics) for helping with the calculations, and Fredrik Almqvist (Umeå University, Chemistry Dept) for advice on organic synthesis.

REFERENCES

1. Geladi P and Åberg P. Three-way modeling of a batch organic synthesis process monitored by near infrared spectroscopy. *J. NIR Spectrosc.* 2001; **9**: 1–9.
2. Smilde A. Comments on three-way analyses used for batch process data. *J. Chemometrics* 2001; **15**: 19–27.
3. Geladi P. Analysis of multi-way (multi-mode) data. *Chemometrics Intell. Lab. Syst.* 1989; **7**: 11–30.
4. Smilde A. Three-way analyses. Problems and prospects. *Chemometrics Intell. Lab. Syst.* 1992; **15**: 143–157.
5. Bro R. PARAFAC: tutorial and applications. *Chemometrics Intell. Lab. Syst.* 1997; **38**: 149–171.
6. Law H, Snyder C, Hattie J and McDonald R (eds). *Research Methods for Multimode Data Analysis*. Praeger: New York, NY, 1984.
7. Coppi R and Bolasco S (eds). *Multiway Data Analysis*. North-Holland: Amsterdam, 1989.
8. Andersson C and Bro R (eds). Special issue. Multiway analysis. *J. Chemometrics* 2000; **14**: 103–331.
9. Allosio N, Boivin P, Bertrand D and Courcoux P. Characterisation of barley transformation into malt by three-way factor analysis of near infrared spectra. *J. NIR Spectrosc.* 1997; **5**: 157–166.
10. Osborne B, Fearn T and Hindle P. *Practical NIR Spectroscopy with Applications in Food and Beverage Analysis* (2nd edn). Longman Scientific and Technical: London, 1993.
11. Burns D and Ciurzak E (eds). *Handbook of Near-infrared Analysis*. Marcel Dekker: New York, NY, 1992.
12. Geladi P, MacDougall D and Martens H. Linearization and scatter correction for near-infrared reflectance spectra of meat. *Appl. Spectrosc.* 1985; **39**: 491–500.
13. Savitzky A and Golay M. Smoothing and differentiation of data by simplified least squares procedures. *Anal. Chem.* 1964; **36**: 1627–1639.
14. Hopkins D. Derivatives in spectroscopy. *Near Infrared Analysis* 2001; **2**: 1–13.
15. Solomons G. *Fundamentals of Organic Chemistry* (2nd edn). Wiley: New York, NY, 1986.
16. Forsström J. *On-line monitoring of the esterification of acetic acid with isoamylalcohol using near infrared spectroscopy and multi-way analysis. Exam Report*, Umeå University, 2000.
17. Fox M and Whitesell J. *Organic Chemistry*. Jones and Bartlett: Boston, MA, 1994.
18. Åberg P. *Multi-way visualisation of NIR and skin-impedance data using PARAFAC. Exam Report*, Umeå University, 1999.
19. Gemperline P, Mouillet V and Serrano D. Software review: Vision, *J. Chemometrics* 2000; **14**: 99–100.
20. *MATLAB Version 5.2 for MacOS*. Mathworks: Natick, MA, 2000.
21. Wise B and Gallagher N. *PLS-Toolbox 2.0 for Use with MATLAB*. Eigenvector Research: Manson, WA, 1998.
22. Meyers R and Montgomery D. *Response Surface Methodology. Process and Product Optimization Using Designed Experiments*. Wiley: New York, NY, 1995.
23. Gurden S, Westerhuis J, Bijlsma S and Smilde A. Modelling of spectroscopic process data using grey models to incorporate external information, *J. Chemometrics* 2001; **15**: 101–121.

